Global Change Biology

Global Change Biology (2015) **21**, 2334–2348, doi: 10.1111/gcb.12855

Design and performance of combined infrared canopy and belowground warming in the B4WarmED (Boreal Forest Warming at an Ecotone in Danger) experiment

ROY L. RICH[1], ARTUR STEFANSKI[1], REBECCA A. MONTGOMERY[1], SARAH E. HOBBIE[2], BRUCE A. KIMBALL[3] and PETER B. REICH[1,4]

[1]*Department of Forest Resources, University of Minnesota, St. Paul, MN 55108, USA,* [2]*Department of Ecology, Evolution and Behavior, University of Minnesota, St. Paul, MN 55108, USA,* [3]*U.S. Arid-Land Agricultural Research Center, USDA, Agricultural Research Service, Maricopa, AZ 85138, USA,* [4]*Hawkesbury Institute for the Environment, University of Western Sydney, Penrith, NSW 2753, Australia*

Abstract

Conducting manipulative climate change experiments in complex vegetation is challenging, given considerable temporal and spatial heterogeneity. One specific challenge involves warming of both plants and soils to depth. We describe the design and performance of an open-air warming experiment called Boreal Forest Warming at an Ecotone in Danger (B4WarmED) that addresses the potential for projected climate warming to alter tree function, species composition, and ecosystem processes at the boreal-temperate ecotone. The experiment includes two forested sites in northern Minnesota, USA, with plots in both open (recently clear-cut) and closed canopy habitats, where seedlings of 11 tree species were planted into native ground vegetation. Treatments include three target levels of plant canopy and soil warming (ambient, +1.7 °C, +3.4 °C). Warming was achieved by independent feedback control of voltage input to aboveground infrared heaters and belowground buried resistance heating cables in each of 72-7.0 m^2 plots. The treatments emulated patterns of observed diurnal, seasonal, and annual temperatures but with superimposed warming. For the 2009 to 2011 field seasons, we achieved temperature elevations near our targets with growing season overall mean differences (ΔT_{below}) of +1.84 °C and +3.66 °C at 10 cm soil depth and (ΔT^{above}) of +1.82 °C and +3.45 °C for the plant canopies. We also achieved measured soil warming to at least 1 m depth. Aboveground treatment stability and control were better during nighttime than daytime and in closed vs. open canopy sites in part due to calmer conditions. Heating efficacy in open canopy areas was reduced with increasing canopy complexity and size. Results of this study suggest the warming approach is scalable: it should work well in small-statured vegetation such as grasslands, desert, agricultural crops, and tree saplings (<5 m tall).

Keywords: canopy temperature, climate change, ecosystem processes, global warming, infrared warming, soil temperature, soil warming, species composition, tree function, trees

Received 7 May 2014 and accepted 2 December 2014

Introduction

Experimentally manipulating temperature in the field remains a logistical challenge for global change scientists (Peterjohn *et al.*, 1993, 1994; Rustad & Fernandez, 1998; Bergh & Linder, 1999; Verburg *et al.*, 1999; Kimball, 2005, 2011; Kimball *et al.*, 2008; Aronson & McNulty, 2009; Kimball & Conley, 2009; and Amthor *et al.*, 2010). A number of approaches exist, each with advantages and disadvantages. The most commonly used techniques include infrared heaters, soil resistance cables, and passively or actively heated aboveground enclosures (Peterjohn *et al.*, 1993, 1994; Harte *et al.*, 1995; Marion *et al.*, 1997; Rustad & Fernandez, 1998; Bergh & Linder, 1999; Verburg *et al.*, 1999; Hollister & Webber, 2000; Wan *et al.*, 2002; Bronson *et al.*, 2008, 2009; Kimball *et al.*, 2008; Aronson & McNulty, 2009; and Hanson *et al.*, 2011). These techniques differ both in regards to how warming is achieved and which ecosystem components are directly targeted by heating (air, foliage, or soils). Differences also exist in whether warming treatment is based on a constant target temperature elevation (Δ°C) (Kimball, 2005, 2011; Kimball *et al.*, 2008) or on a constant energy input (watts per m^2) (Harte *et al.*, 1995). The approaches differ in their effects on temperatures, relative humidity, foliage boundary conditions, and soil moisture (Bronson *et al.*,

*Correspondence: Roy L. Rich, tel. +651 328 4391, e-mail: rich0475@umn.edu

2008; Kimball, 2011). They also differ markedly in infrastructure investment and ease of deployment.

Chamber-based manipulations have concurrently warmed aboveground and soil and shown warming influences on ecological processes such as soil respiration rates, phenology, bud burst, and shoot elongation in boreal spruce plantations (Bronson *et al*., 2008, 2009). However, there is concern about the chamber-based approach because of the separation of enclosed ecosystems from the surrounding environment and the additional logistics and expense needed to mitigate chamber effects on diurnal warming patterns (Bronson *et al*., 2008, 2009). In contrast to the chamber-based dual aboveground and belowground warming, free-air aboveground infrared heater-based warming, and belowground resistance cable-based warming are frequently but independently used methods (Peterjohn *et al*., 1993, 1994; Harte & Shaw, 1995; Rustad & Fernandez, 1998; Bergh & Linder, 1999; Verburg *et al*., 1999; Kimball, 2005, 2011; Kimball *et al*., 2008). Because of the logistical complexity, expense, and high-energy requirements, all free-air experiments to date have focused on heating either aboveground or belowground, but not both. Aboveground feedback-controlled warming manipulation alone has become more common in a variety of ecosystems, such as tundra (Nijs *et al*., 2000), grazing land (Luo *et al*., 2010), paddy rice (Rehmani *et al*., 2011; Gaihre *et al*., 2014), rangeland (Morgan *et al*., 2011; LeCain *et al*., 2014), soybean (Ruiz-Vera *et al*., 2013), wheat (Wall *et al*., 2011; Ottman *et al*., 2012), and on tree seedlings (McDaniel *et al*., 2014). While infrared heaters warm vegetation and exposed soil surfaces, associated soil temperature elevation often diminishes with depth (Luo *et al*., 2010), is less effective when soil moisture is higher (Wall *et al*., 2013; McDaniel *et al*., 2014), and fluctuates diurnally relative to ambient soil.

Warming of soils via aboveground infrared heaters is likely to be less effective in densely vegetated ecosystems, where canopy interception of radiation (which prevents it from directly reaching the soil surface) is greater than re-radiation downward from warmed vegetation. For example, Luo *et al.* (2010) measured soil warming effects to 40 cm and found that the effect of warming diminished with depth under conditions of high vegetation cover (no-grazing treatments). Hence, simultaneous belowground and aboveground heating may be useful to achieve additional heating throughout the soil profile as compared to aboveground-only experiments, especially in ecosystems without a large fraction of bare ground or where cross winds could carry away much of the energy before it reaches the soil surface. Additionally, IR heater effects are diminished midday by wind and in vegetation with high leaf area index and/or high evapotranspiration (Kimball, 2005; Kimball *et al*., 2012a; and Wall *et al*., 2013). Thus, warming belowground may compensate somewhat for these limitations as well as energy losses to surrounding ambient temperature soils. Lastly, soil heat flux represents an important and often overlooked source of incident radiation, especially for understory plants, where it may account for 30–50% of net radiation (Ogée *et al*., 2001; Ochsner *et al*., 2007).

Herein, we describe the rationale for the design, implementation, and performance of a simultaneously imposed temperature free-air controlled enhancement (T-FACE) aboveground (infrared heating) treatment and a belowground (resistance cable heating) warming experiment on tree seedlings, which, to our knowledge, has not been attempted previously. The experiment, named Boreal Forest Warming at an Ecotone in Danger (B4WarmED), addresses the potential for projected climate warming to alter tree function, species composition, and ecosystem processes at the boreal-temperate forest ecotone (Sendall *et al*., 2014; Reich *et al*., 2015). Diverse woody ecosystems are among the most challenging places to conduct warming manipulations, because the structural variation of herbaceous and woody plants creates a spatially heterogeneous canopy, complicating the control of temperature elevation compared with similar experiments that target monocultures of even-aged short-statured vegetation, such as agricultural crops. The warming apparatus and control were designed to maintain a fixed temperature elevation above ambient canopy and soil temperatures in 3 m diameter plots, and thus simulate the diurnal and seasonal patterns to be experienced in the future by juvenile trees and the matrix of naturally occurring ground layer vegetation and soils in which they grow.

Materials and methods

Study sites

The warming facility was installed at two sites, ~150 km apart, in forests that span the transition from temperate to boreal biomes in northern Minnesota, USA. One site was located at the Cloquet Forestry Center (CFC), Cloquet, MN, USA (46°40′46″ N, 92°31′12 W, 382 m a.s.l., 4.5 °C mean annual air temperature (MAT), 807 mm mean annual precipitation), and the other higher latitude site was at the Hubachek Wilderness Research Center (HWRC) near Ely, MN, USA (47 56′ 46″N, 91°45′29″W, 415 m a.s.l., 3.0 °C MAT, 722 mm mean annual precipitation). At both sites, the warming infrastructure is located on coarse-textured upland soils in 40- to 60-year-old mixed aspen–birch–fir stands scattered with pine, spruce, and other species. Sites were chosen from stands of mixed aspen forests for their size (>6 ha), canopy and topographic similarity, and their proximity to electrical power infrastructure. Plots were located in both closed canopy (≈5–10% of full sun-

light) and open overstory (≈80% of full sunlight) conditions. We included both closed and open plots because regeneration in closed canopy and recently disturbed habitat types is important in shaping boreal forest canopy composition, given the spatial and temporal patterns of natural and anthropogenic disturbances (Heinselman, 1973; Grigal & Ohmann, 1975; Frelich & Reich, 1995). Initial site development occurred in 2007 and 2008 and included dividing stands into six experimental blocks. Blocks designated as open canopy sites were harvested, and stumps were cut to less than 30 cm height in winter 2006 and 2007 for Cloquet and early spring 2008 for Ely. All blocks were brush cut by hand to remove tree saplings and shrubs. Individual plots were established by selecting patches of level ground at least 1 m from canopy trees or remaining stumps. Individual plots were located in proximity to one another but no closer than 2 m apart to facilitate the delivery and monitoring of warming treatments.

Experimental design

The experimental design is a 2 (site – CFC and HWRC) × 2 (habitat – open and closed overstory) × 3 (warming – ambient, +1.7 °C, and +3.4 °C) factorial, with six replicates (2 per block) for a total of 72–7.1 m^2 circular plots (Fig. S1). Within each plot, 121 seedlings of 11 tree species were planted into the remaining herbaceous vegetation in a gridded design. Originally, the experimental design included an additional control group without infrared heating and without buried cables as a check for possible biological impacts of soil disturbance associated with burying cables. As these plots were unheated, and after 2 years of testing did not differ thermally or biologically from the ambient plots with cables (data not shown), they will not be discussed further. The warming treatments included two target levels of simultaneous plant and soil warming (+1.7 °C, +3.4 °C) chosen to bracket the anticipated warming approximately 75–100 years from now (Kling *et al.*, 2003; IPCC, 2013; Handler *et al.*, 2014) and to enable assessment of nonlinear responses to warming.

Belowground warming was accomplished through buried resistance-type heating cables (146 m, 240V VAC, Danfoss-GX, Devi A/B, Denmark; Peterjohn *et al.*, 1993; Bergh & Linder, 1999). In early spring 2008, the cables were installed by hand at a depth of 10 cm and spaced 20 cm apart in an east to west orientation giving a maximum heating capacity of approximately 153 Wm^{-2}. Slit trenches for the cable were dug by hand or carbide tipped chainsaw (Fig. 1). For ambient plots, a PVC tube, whose diameter matched the resistance cable sleeve, was buried to emulate the soil disturbance of the warmed treatments.

Aboveground heating was achieved by installing a T-FACE system following established methods in Kimball *et al.* (2008) with some adaptations to the forested ecosystem and treatment levels. Ceramic heating elements (Model FTE-1000, 240V, 245 mm × 60 mm; Mor Electric Heating Assoc., Inc., Comstock Park, MI, USA) warmed aboveground structures. Six elements oriented in hexagonal pattern provided a heater capacity of 499 Wm^{-2} $°C^{-1}$ for +1.7 °C, while eight elements oriented in an octagonal pattern provided a capacity of 333 Wm^{-2} $°C^{-1}$ for +3.4 °C treatments (Fig. 1). These values are for the electrical energy input, whereas the infrared radiant output was on the order of 30% of these values depending on wind speed (Kimball *et al.*, 2008, 2012a,b). The heaters were mounted at 45° from horizontal using a ball mount (Panavise Products Inc., Reno, NV, USA) on a steel tube crossbar and were set to an initial height of 1.6 m attached to channel posts located 10 cm outside the plot edge (Fig. 1). All ambient plots also had posts, crossbars, and dummy heaters oriented in the same manner.

Monitoring and control

We used a unified integrated microprocessor-based feedback control based on maintaining a fixed temperature differential between warmed and ambient control plots with targets of either +1.7 °C or +3.4 °C (Fig. S2). Aboveground and belowground temperatures were monitored at each plot continuously (and logged at 15-min intervals). In 2009 and 2010, canopy temperatures were measured with infrared thermometers with an 18° field of view mounted at a height of 1.6 m above the soil surface and tilted 35° from nadir at the southern edge of each plot (IRR-P: Apogee Instruments Inc., Logan, UT, USA). In 2011, these radiometers were reoriented directly over the plot at a height of 1.85 m above the soil surface to maximize the viewing area and to accommodate the growing forest canopy. Sensors were recalibrated or replaced periodically as needed. For belowground temperature measurement within

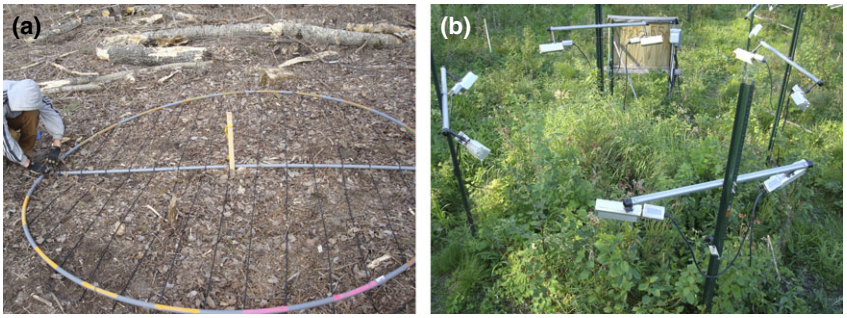

Fig. 1 (a) Pattern and placement of soil cables prior to being inserted 10 cm belowground, (b) Example open +3.4 °C canopy plot in 2010.

each plot, two sealed thermocouples (type T) were installed at 10 cm depth located 6.6 cm from the nearest cable; as a supplement, in 2010, we added thermocouples at 20, 30, 50, 75, and 100 cm depths at a distance ~1 m from the outside edge of a subset of plots. Volumetric water content from 0 to 20 cm depth was monitored in each plot using a 30 cm Campbell Scientific CS-616 probe inserted at 45°. All sensors were connected via AM16-32 or AM25T multiplexers to a Campbell Scientific CR-1000 data logger at each block (Fig. S2). Overall, we had 475 sensors deployed at the two sites. For clarity, unless explicitly stated as air temperature, all reported measures for aboveground temperatures are for foliage temperature measured by infrared radiometer; all belowground temperatures are measured by thermocouples places at 10 cm depth unless another depth is specified.

Each site was also equipped for measuring precipitation [MET-One model 385AC from Campbell Scientific (CS), Logan, UT, USA], wind speed and direction (R.M. Young 03002-L Wind and sentry set – from CS), net solar radiation (LI200X via Licor Biosciences, Lincoln, NE, USA), and photosynthetically active radiation in both the open and closed canopy (LI190SB via Licor Biosciences). Ambient air temperature sensors (type T thermocouples with radiation shields) were deployed at the block scale (at 1 m height). In 2011, additional ambient air temperature and relative humidity (HMP60 from CS) probes were installed in both canopy conditions at 1.5 m height. In 2010 and 2011, short duration, high intensity supplemental measurements were made to measure temperature heterogeneity within individual plots. Aboveground measurements included sampling air temperature at eight heights (every 25 cm from 25 to 200 cm above each soil surface) at 12 locations within each plot located 50 or 100 cm from the plot center. Additionally, in 2010, FLIR images were taken to visualize the distribution of IR-warming within a subset of plots at CFC (Fig. 2).

Supplementary measurements of belowground warming uniformity included north–south-oriented transects (perpendicular to warming cable installation direction) of 16 or 32 thermocouples spaced every 2.5 cm at 10 cm depth. Horizontal variation in soil warming (at 10-cm depth) was low as measured by the deviance of each measurement point from mean soil temperature at each plot; the absolute value of deviance rather than raw temperature was used because measurements for differing plots were taken at differing times. The absolute value of the deviance values was 0.10° (0.17 standard deviation) for T_{amb}, 0.78° (0.09) for $T_{1.7}$, and 0.13° (0.10) for $T_{3.4}$.

Feedback control was executed every 10 s at the block scale by maintaining a targeted difference (+1.7 °C or +3.4 °C) between the average canopy temperature of ambient replicates and that of each individual warmed plot in each block. Data loggers (Model CR1000 from CS) were programed to modulate dimmers (Kaglo Inc., LCEDT-24168 or LCEDT-2484, Bethlehem, PA, USA) controlling IR heater voltage or soil voltage under a proportional–integrative–derivative (PID) control system where wattage fluctuates dynamically to maintain temperature treatments (Kimball, 2005). Model SDM-CV04 current–voltage interfaces generated 0–10V control signals to control the dimmers. To maintain even temperature differences between soil resistance cables, voltage to soil warming cable was kept below 40% of total voltage capacity (96 V).

Contingency programing was implemented, allowing for sensor data from neighboring plots of the same treatment type

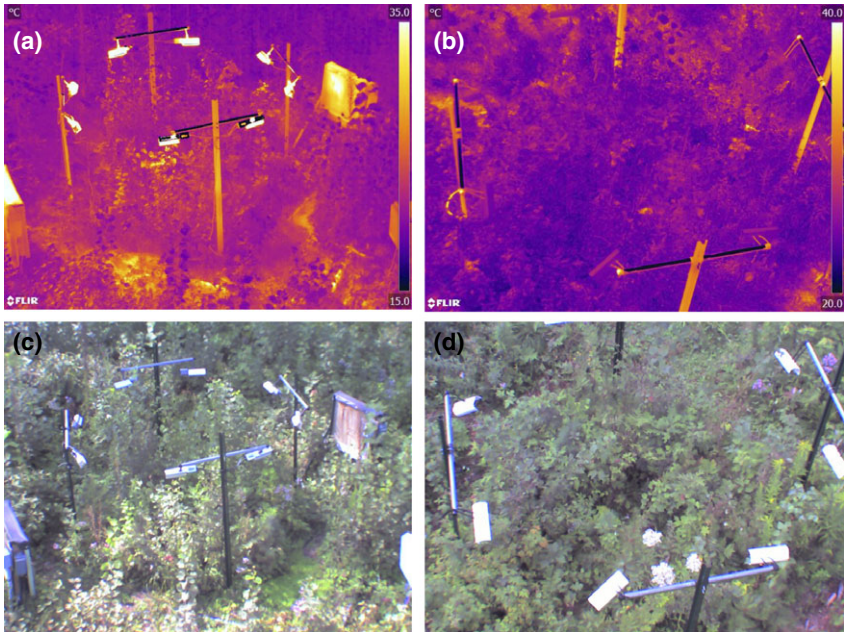

Fig. 2 The FLIR of open canopy (a) +3.4°or (b) ambient plots at CFC site in 2010. FLIR image scales have been set so that ambient foliage temperature corresponds to the same color in each image. Corresponding visual images of open canopy (c) +3.4° or (d) ambient plots.

to be used as substitute data when sensors were offline or out of range. High wind thresholds were also put in place to conserve energy that limited heater power consumption to 64% when wind speeds were greater than 5 m s^{-1} and turned off when winds exceeded 10 m s^{-1}. From the day of year 181 in 2011 to the day of year 261 in 2012, a programing error defaulted limits to 80% of voltage capacity (64% of power) across all plots on both sites during those days.

Soil moisture

Infrared warming of vegetation increases the vapor pressure gradient from inside the leaves to the air, so increased evaporative demand occurs. To compensate, Kimball (2005, 2011) suggested adding supplemental irrigation in amounts calculated to make infrared warming experiments more similar to global warming at constant relative humidity (Wall *et al.*, 2011). However, as climate warming is likely to increase the vapor pressure deficit, and thus result in increased soil water deficits, we believed that adding water would make our experiment less realistic and therefore did not do so. This approach is consistent with recent data and models that suggest that total vapor content does not increase fast enough to keep pace with increased warming over land; decreases in relative humidity, and more importantly, significant increases in vapor pressure deficit are key signatures of climate warming over land (Sherwood & Fu, 2014). Volumetric water content (cm^3 H_2O/cm^3 soil) was monitored hourly in all plots and corrected for soil textural and temperature differences using a Campbell Scientific method for user-specific calibration of water reflectometers (Model CS616 from CS).

Warming duration

Current and prior warming experiments in cold-winter ecosystems vary in whether or not they maintain warming treatments throughout the winter (e.g., Harte *et al.*, 1995; Verburg *et al.*, 1999; Bronson *et al.*, 2008). Although warming in winter can have important impacts on ecosystem processes, the low levels of biological activity at <0 °C, the potential artifacts of our warming treatments on snow melt and freeze/thaw cycles, and the high expense of warming year-round in aggregate led us to decide not to warm in winter. Moreover, ambient plot soil data show that soil temperature disassociates with air temperature during winter months, probably due to snow cover. At 10 cm below the surface, temperature is stable at −2 to 0 °C throughout the winter with changes in temperature coming only after snow melt.

Turn-on and turn-off dates were dictated by prevailing weather conditions, namely when ambient air temperatures were greater than 1 °C, based on 24-h average for more than five consecutive days during the shoulder seasons. Our warming season (henceforth referred to as field season) ranged from 208 to 244 days per year (Table 1). The field season was shorter in all years at HWRC. Consistent with historical data showing lower MAT near HWRC, we observed slightly lower (by 0.6 °C on average) MAT near HWRC. However, mean temperatures during the field season were slightly higher at HWRC (by 1.4 °C on average), because of the shorter field season length (by 17 days on average) at that site (Table S1).

Data processing

We removed values that were out of range due to sensor malfunction or error and filled missing values to generate a continuous data set across all plots to characterize treatments and for use with biological measurements. From 2009 to 2011, missing sensor data accounted for 4.1% of aboveground and 3.6% of belowground hours logged. The longest increment of time that sensor data were missing for any given plot was 6 days. Sensor malfunction and miscalibration detection were systematically based on observed patterns of malfunctioning

Table 1 Summary of aboveground foliage and belowground (10 cm depth) warming treatment average temperatures (°C), and volumetric water content averages (cm^3 H_2O/cm^3 soil) for 2009–2011 field seasons (nonfrozen days when the warming treatment was implemented). Ambient treatments (*T*) along with differences (Δ) from ambient for +1.7° and +3.4° treatments are reported. Aboveground and belowground data are differentiated by superscript and subscripts, respectively.

	Year	2009				2010				2011			
	Site	CFC		HWRC		CFC		HWRC		CFC		HWRC	
	Canopy	Closed	Open	Closed	Open	Closed	Open	Closed	Open	Closed	Open	Closed	Open
	Warmed days	237		208		244		236		225		210	
Above	$T_{ambient}$	10.46	11.33	11.08	12.25	11.73	12.12	11.80	12.69	11.59	11.97	12.73	13.09
	$\Delta^{1.7}$	1.87	1.92	2.00	2.10	1.90	1.85	2.06	1.96	1.79	1.78	1.82	2.27
	$\Delta^{3.4}$	3.70	3.50	3.68	3.86	3.74	3.66	3.78	3.78	3.46	3.37	3.47	3.88
Below	$T^{ambient}$	10.41	10.48	11.40	11.80	11.37	11.26	11.86	12.27	11.08	11.01	12.86	13.01
	$\Delta_{1.7}$	2.11	1.94	2.10	1.76	1.99	1.79	2.21	1.63	1.60	1.50	1.78	1.38
	$\Delta_{3.4}$	4.01	3.40	3.94	3.69	3.71	3.21	4.09	3.43	2.93	2.73	3.28	2.96
	$VWC_{ambient}$	0.23	0.24	0.30	0.16	0.23	0.24	0.28	0.16	0.22	0.23	0.25	0.13
	$VWC_{1.7}$	0.21	0.20	0.27	0.15	0.21	0.21	0.25	0.16	0.19	0.19	0.22	0.13
	$VWC_{3.4}$	0.20	0.19	0.24	0.13	0.20	0.18	0.23	0.13	0.18	0.18	0.21	0.11

sensor data. Both infrared radiometer and thermocouples were observed to exhibit increased variability when malfunctioning.

Along with error logs, we detected malfunctioning sensors in our 15-min average data by comparing sensor measurements of temperature at each time increment regardless of treatment. We calculated trimmed means and trimmed standard deviations among all plots at block scale to minimize microenvironmental variation; we used the value 0.13, to trim the maximum and minimum observation. A trimmed mean was necessary due to very high or low values that skewed the mean and inflated the standard deviation making detection of faulty sensors unlikely. We removed individual sensor values when they were more than two standard deviations from the trimmed mean at any given time increment. Additionally, we limited data to within the range of temperatures observed over the field season. For belowground, this was −11 to 46 °C, and for aboveground, it was −15 to 46 °C. Altogether, this processing removed an additional 1.1% of values for aboveground and 3.1% of total values for belowground.

We detected out of calibration but functioning sensors by comparing plots within individual treatments by each site–canopy combination over monthly increments to look for systematic differences in sensor performance among plots that should behave similarly. We compared average values for each plot within each treatment type to the median of all similar treatment replicates in each site–canopy combination. Individual sensor values were compared with the median value because miscalibrated sensors were observed to skew the mean. Variation in sensor values was reduced by aggregating the data, so sensors with values more than ±1 SD from the median were flagged for omission. As a check on this approach, we visually inspected individual plot data for abrupt shifts in temperature patterns indicative of sensor misplacement or miscalibration and compared plot temperature readings with power output. We crosschecked this approach by looking for shifts in sensor performance (e.g., a jump to a new level) that could not be explained by power shifts or environmental changes and were not corrected by regular sensor maintenance regimes. For example, an individual ambient plot sensor would be omitted if it began to read systematically higher values than nearby warmed treatments over several weeks. Omitted data accounted for an additional 3.1% aboveground and 1.4% belowground of total hourly data points.

Missing or removed values (total = 8.3% aboveground and 8.1% belowground) were filled to make a continuous data set across all plots for use in analyses of biological responses. Missing data were filled at the hourly time increment scale; if an individual plot was missing data, it was replaced with values from the nearest replicate of the same treatment. In most cases, data were filled with temperature data from a replicate in the same block. If a suitable replicate within the block was missing, the mean value from the site x canopy average for a given treatment was used. In 2011, 0.06% of data points from ambient open plots were filled using data from closed canopy plots by predictions from a regression model of open vs. closed canopy temperature because the ambient sensors had a programing error.

In this study, calculations of energy use are based on the 15-min average of power control output to SDM-CV04 interfaces that generated voltage signals to the dimmers. Our data collection from 2009 to 2011 included the arithmetic mean PID output signal over each 15-min interval, which was used to calculate power consumption. We did not store the quadratic mean (PID output signal^2) over each interval, which would be necessary for a precise calculation of wattage output based on the voltage. We report our results as kWh/m^2, but this value is likely lower than the true kWh/m^2. Power costs for the experiment averaged $2059 per plot/yr, and we paid $0.10 per kWh (Table S2).

Statistical analysis

We used linear mixed models with residual maximum likelihood (REML) (Table 2) to evaluate the treatment effects vs. other aspects of the experimental design, using temperature differences, ΔT^{above} and ΔT_{below}, as response variables (henceforth, superscripts or subscripts differentiate common

Table 2 Summary of mixed models with residual error maximum-likelihood portioning for ΔT_{below} and ΔT^{above} responses. Models shown are field season scale aggregations of data but correspond to results at hourly and daily scales. DFDen, degrees of freedom used in denominator of each test (n-k-1)

Response	$\Delta_{belowground}$		$\Delta^{aboveground}$	
RSquare	0.99		0.97	
RSquare Adj	0.99		0.97	
Root mean square error	0.14		0.27	
Mean of response	1.87		1.77	
Observations	432		432	
Random effect	Variance component	Percent of total	Variance component	Percent of total
Plot [treatment_abbr, site, canopy]	0.0099	27.78	0.0071	7.69
Block [site, canopy]	0.0068	19.17	0.0123	13.25
Residual	0.0188	53.06	0.0734	79.06
Total	0.0355	100	0.0928	100
Fixed effects	df DFDen	*F* ratio	Prob > *F*	F Ratio	Prob > *F*
Treatment_abbr	2 58	6205.49	<0.0001	3781.30	<0.0001
Site	1 9	4.40	0.07	0.97	0.35
Canopy	1 9	0.45	0.52	8.99	0.02
Year	2 357	11.71	<0.0001	89.05	<0.0001
Daylight	1 357	7.58	0.01	109.23	<0.0001

2measurements aboveground or belowground). Models included the fixed effects of site, canopy, treatment, day vs. night, and year; random effects included block and plot (nested in site, canopy, and treatment). In this study, only unfilled data were used for statistical analysis. We calculated ΔT^{above} and ΔT_{below} from 15-min average data summarized to hourly averages. Any subsequent data aggregations are based on hourly averages summarized to various time increments.

Results

Across 3 years of operation (2009–2011), we achieved consistent differences between ambient, +1.7 °C, and +3.4 °C treatments aboveground and belowground in both sites under both canopy conditions (Table 1, S3, Figs 3–5). Moreover, seasonal temperature distributions aboveground and belowground in treated plots matched those in ambient plots (Figs 3, 6, and 7). From 2009 to 2011, hourly warming season ambient air temperatures ranged from −14.9° to 36.6° C at CFC and −11.7° to 38.4 °C at HWRC. Aboveground plant temperatures from IR radiometers ranged from −15.0° to 35.8 °C at CFC and −13.9° to 40.0 °C at HWRC. Ambient soil temperature (at 10 cm) ranged from −0.3° to 23.9 °C at CFC and −0.2° to 24.8 °C at HWRC (Table 1, Figs 1–3). At the field season scale, our temperature elevations were near our targets of +1.7 °C and +3.4 °C (Table 1, S3, Figs 3–5). Model fits show warming treatments as the dominant effect established by the experiment compared with either random or other fixed effects. For the part of the year warming treatments were deployed, we found no significant differences in ΔT^{above} and ΔT_{below} between sites. In contrast, we did find significantly lower ΔT^{above}, but not ΔT_{below}, in open vs. closed canopy areas (Table 2).

Seasonally and across years, in open canopy areas, increasing canopy complexity and higher evapotranspiration created by growing vegetation resulted in a need for additional energy to reach the target temperature elevations (Fig. 8 gives an example of one site in 1 year). Sometimes, insufficient energy output was available to reach the target, for example, treatments often were close to, but below, target elevations at midday in midsummer in open plots (Fig. 9). We also found year to be a significant effect, with 2011 having lower ΔT^{above} than 2009 or 2010. The 2011 difference can be attributed in part to a programing glitch that limited power output during the second half of the growing season. However, greater power output was still needed for 2011 prior to the programing glitch than in other years for that same common period (days 135–181). Mixed models run for this same period of time show year remains a significant effect.

There were significant differences in how ΔT^{above} varied diurnally and seasonally. For example, daytime ΔT^{above} was significantly lower than nighttime ΔT^{above}. This difference was weak but significant for ΔT_{below} as well. Differences in day vs. nighttime ΔT^{above} were less pronounced in closed vs. open canopy (Fig. 9). In general, aboveground treatment stability and control were greater during the nighttime than daytime and in closed vs. open canopy sites (Fig. 5). Effectiveness of aboveground plant warming declined in midday as achievable ΔT^{above} decreased with mean temperature concurrent with peak power use (Fig. 9). ΔT^{above}

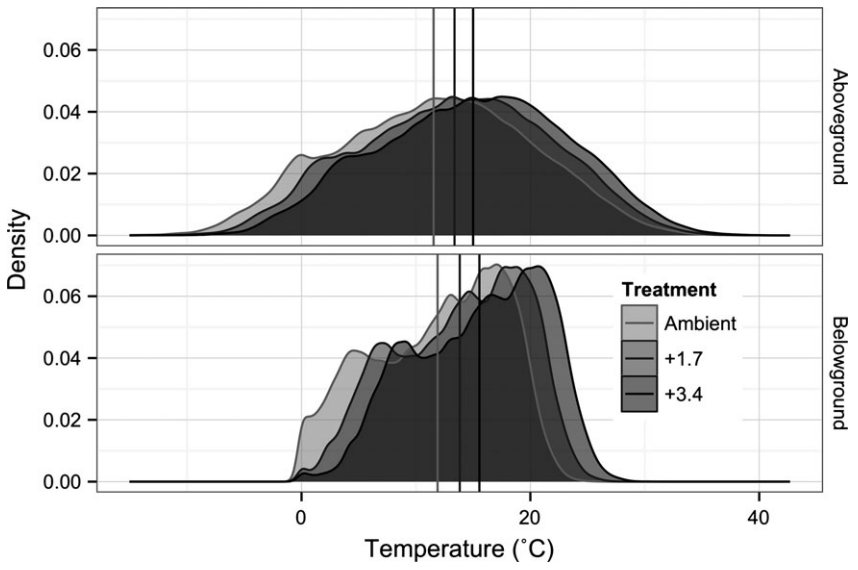

Fig. 3 Density plot of complete hourly aboveground (foliage) and belowground (at 10 cm depth) 2009–2011 field season temperatures in ambient (lightest gray), +1.7 °C (medium gray), and +3.4 °C (dark gray) treatments. Vertical reference lines are overall means.

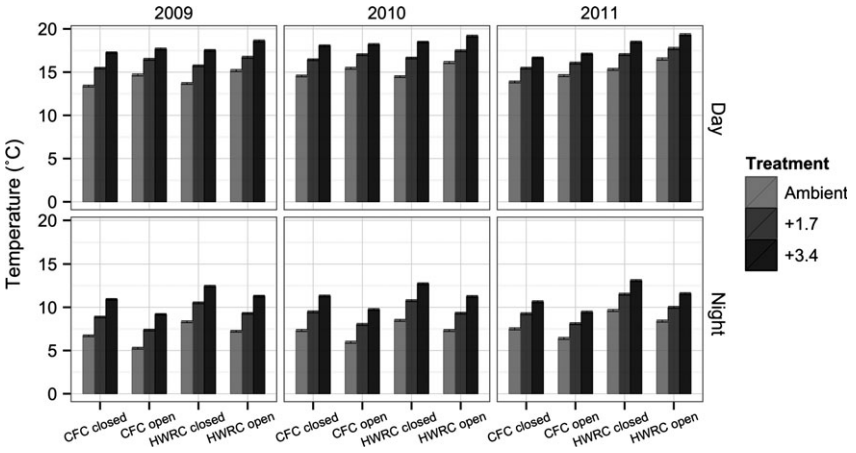

Fig. 4 Average field season aboveground foliage temperature (°C) for T^{amb} (light gray), $T^{1.7}$ (medium gray), and $T^{3.4}$ (dark gray) by year and daylight condition for HWRC and CFC sites (with 95% CI bars).

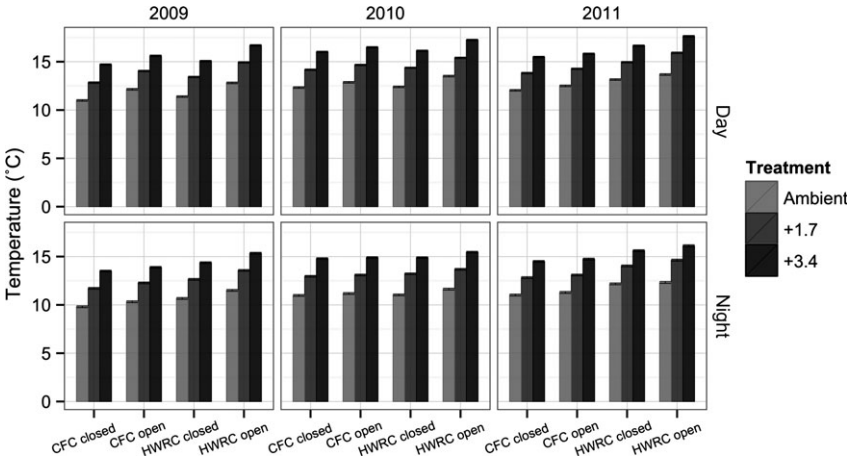

Fig. 5 Average field season belowground (10 cm depth) temperature (°C) for T_{amb} (light gray), $T_{1.7}$ (medium gray), and $T_{3.4}$ (dark gray) by year and daylight condition for HWRC and CFC sites (with 95% CI bars).

generally decreased with increasing ambient foliage temperature. Thus, seasonally, ΔT^{above} was lowest in the month of August each year.

Belowground soil temperature treatment differences were diurnally stable relative to aboveground treatments (Fig. 9). Soil temperatures were most variable in the beginning of each field season, when lack of foliage resulted in IR heaters warming soils beyond treatment targets. Soil temperature profiles showed that the magnitude of soil warming declined with depth (20–100 cm) but warming treatment had an observable effect at the deepest depth monitored (+1.6 °C for the $T_{3.4}$ at 100 cm) (Table 3, Fig. S3). Volumetric water content (VWC, cm^3 H_2O/cm^3 soil) was reduced by roughly 10% at +1.7 °C and 20% at +3.4° on average from 2009 to 2011 (Table 1, Fig. S4). Generally, these differences in VWC increased with time since precipitation and through the growing season.

The pattern and efficiency of aboveground IR plant warming has been well established for experimental configurations similar to our design (Kimball *et al.*, 2012a,b) but not for a mixed species tree seedling and ground layer community. Supplementary data from FLIR images and air temperature profiles within plots showed only modest differences between ambient and heated plots in aboveground spatial patterns of temperature. FLIR images taken in 2010 of ambient plot, and heated plots were visually similar (Fig. 2). A digital analysis of images quantified the range of variation in surface temperature in horizontally vs. vertically oriented dimensions based on data from pixels intersecting 1 m long lines (FLIR Tools, FLIR Systems Inc., Wilsonville, OR, USA). We found no statistically significant differences in horizontal vs. vertical dimensions for temperature range observations. Warmed (+3.4 °C) plots had a larger range in temperature within plots,

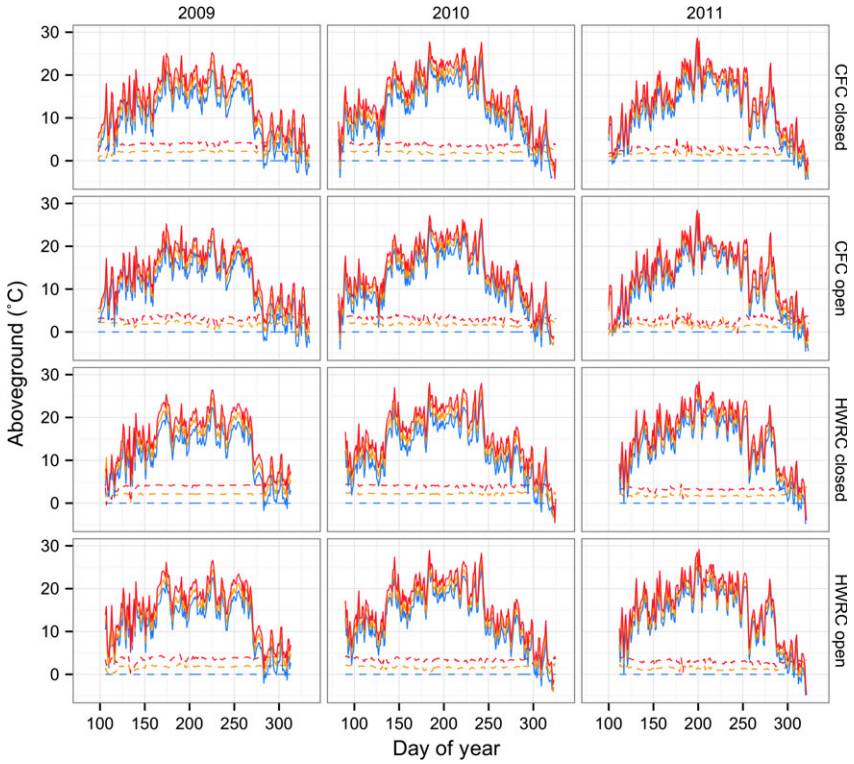

Fig. 6 Average daily aboveground foliage temperature (solid line) and ΔT^{above} (dashed) for T^{amb} (blue), $T^{1.7}$ (orange), and $T^{3.4}$ (red) treatments by day of year by year and site x canopy condition.

but these data are not conclusive given our small sample size (Table S5).

As FLIR images only measure surface temperatures, a 3-dimensional grid of air temperature sensors was periodically deployed within individual plots to assess spatial heterogeneity (as well as whether air temperatures matched or differed from plant surface temperatures). These observations were limited to four ambient and four elevated plots. Air temperature at all heights in warmed treatments was elevated across the height profile (Fig. S5). Mean weekly air temperature elevations were variable and ranged from 0.75° to 1.92 °C for $T^{1.7}$ treatment and 0.77° to 2.52 °C for $T^{3.4}$° treatment; this variation results from differential capacity to re-radiate heat of vegetation during different times of year and also wind speed. Patterns of ambient and warmed air temperature were similar but more differentiated across height in warmed plots (Fig. S5). Additionally, comparison of inner (50 cm from plot center) vs. outer regions (100 cm from plot center) shows modest differences (<0.25 °C) (Fig. S5).

Discussion

Overall, the B4warmED approach was able to successfully warm plots to near our targets of +1.7° and +3.4 °C warmer than their surroundings both aboveground and belowground, without use of chambers. Our results thus show that this system can be used effectively to raise temperatures in low forest vegetation in a fashion that maintains temporal variability patterns at daily, seasonal, and yearly time frames. Here, we address the technical and environmental challenges of warming forest vegetation and the implications of our results.

Technical challenges and solutions

The scale of this experiment presented challenges to efficient operation, such as those related to maintaining an extensive experimental infrastructure, including the feedback control system, sensor arrays, and controllers. As problems and inefficiencies were encountered, modifications were made to the experimental operation. A key issue for this experiment was the logistics of maintaining 475 individual sensors in working order without skewing the performance of feedback control based on those sensors. The challenge of maintaining infrared radiometers in optimal order was particularly vexing as they required frequent recalibration and had frequent failures exhibited as measurement variability or base level shifts in observed temperature. Control

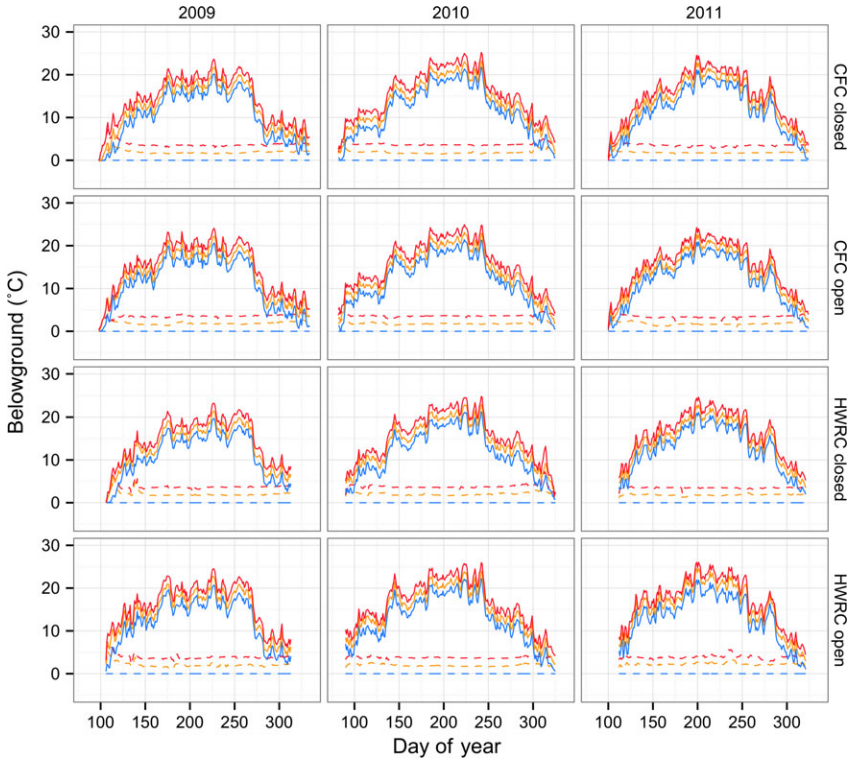

Fig. 7 Average daily belowground (10 cm depth) temperature (solid line) and ΔT_{below} for T_{amb} (blue), $T_{1.7}$ (orange), and $T_{3.4}$ (red) treatments by day of year by year and by site × canopy condition.

program alterations included code for detection of problematic sensor performance based on data variability and range. Problematic sensors were isolated from the feedback control aspects of the program and flagged for maintenance. This programing code could be implemented manually or automatically and was key to a robust warming system.

In the first 1.5 years of the experiment, heater element failure was frequent and related to the frequency of controller voltage shifts. Based on an improved algorithm from the SoyFACE project (Ruiz-Vera *et al.*, 2013), we modified the original feedback control program to provide more gradual shifts in heater output and to improve experimental heating performance specific to our plots. We introduced code for adjustment of power output to heaters based on 1-min projection of power needs, derived from the observed rate of change in heated foliage temperature relative to the observed rate of change in ambient foliage temperature given the current power output. These changes led to a more consistent coupling of controller output to *in situ* foliage conditions and more gradual shifts in IR heater output (Table S4 contains example code used to program feedback control).

Efficient operation and the logistics of having two field sites 150 km apart demanded that program control for both sites be accessible online, enabling problems as well as routine diagnostics and heating controls to be addressed remotely. Additional program modifications for efficiency included writing a universal program framework ('Sauron') that operated any of the 12 data loggers on the two sites, thus allowing for any program changes to be implemented uniformly and efficiently.

Our experimental operation was technically challenged by issues related to the AC power equipment components. Primarily, our voltage controllers (Kaglo manufactured dimmers) proved problematic because their components (specifically the thyristor and voltage transformers) created harmonics in our electrical grid and interference in our data logger communication network, which was likely exacerbated by the quantity (48) used at each site. This problem necessitated the conversion of our communication system from a wired to a radio network. In 2012, when these dimmers began to fail more often, the replacement of all Kaglo dimmers with solid state control relays eliminated harmonics (Model MCPC2450C, Crydom Inc., San Diego CA, USA).

Environmental challenges

Feedback control of warming for a heterogeneous seedling canopy proved to be challenging at several scales of control. Growth and phenological differentiation

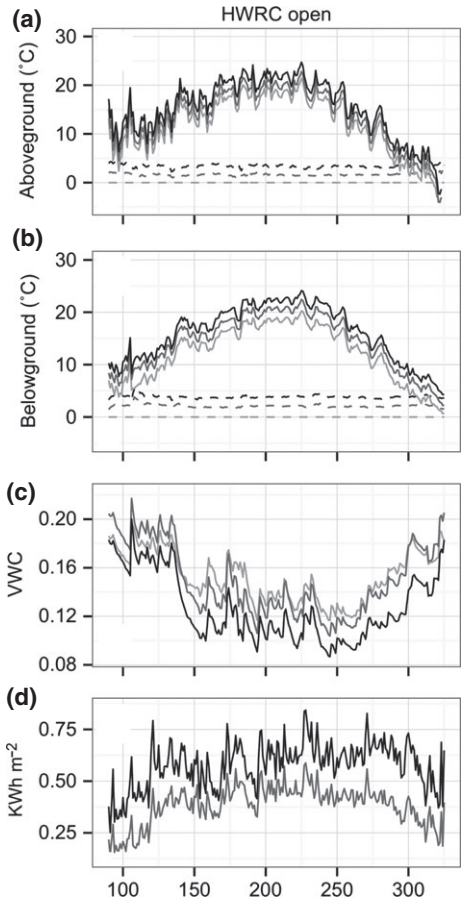

Fig. 8 Seasonal data from HWRC 2010 field season by day of year: (a) aboveground foliage temperature (solid line) and ΔT^{above} (dashed) for T^{amb} (light gray), $T^{1.7}$ (medium gray), and $T^{3.4}$ (dark gray) treatments; (b) belowground temperature at 10 cm depth (solid line) and ΔT_{below} for T_{amb}, (light gray), $T_{1.7}$ (medium gray), and $T_{3.4}$ (dark gray); (c) volumetric water content (cm^3 H_2O/cm^3 soil) for T_{amb}, (light gray), $T_{1.7}$ (medium gray), and $T_{3.4}$ (dark gray); and (d) Estimated KWh $m^{2\ -1}$.

among the ambient, +1.7°, and +3.4° treatments caused difficulty in standardizing the infrared radiometer viewing area between heated and reference plots. Individual seedlings also grew into positions where they could dominate the sensor field of view. Phenological differences in leaf expansion and senescence also created ephemeral asynchrony in the radiometer field of view due to the ratios of exposed soil vs. brown vs. green vegetation. Differential growth created an additional challenge as shade intolerant species grew much faster than other species and thus outgrew the experiment's expected 2.2 m height sooner than slower growing shade tolerant species. Frequent adjustments of the infrared radiometers were necessary to maintain similar foliage areas observed and an equivalent position relative to the seedling canopies. Heater heights were raised throughout the experiment in accordance with the predominant seedling canopy height in each plot and were raised higher earlier in open canopy blocks.

Shifting light environments also made defining ambient and elevated temperature control problematic as incoming solar radiation increased foliage temperature rapidly. The differences in light environment resulted in short duration shifts in temperature among ambient and treatment plots. For example, an ambient plot in a sun fleck could be temporarily warmer than a warmed plot in the shade and thus had the potential to overwhelm the warming capacity of our heaters as they tried to compensate for the differing light environments. This effect contributed to higher ΔT^{above} variation during the midday, particularly in the closed canopy plots. To fully mitigate this effect on a minute-by-minute basis, ambient plots serving as the basis of feedback control would have to shift dynamically with the current light environment in warmed treatments.

As has been seen in other aboveground infrared arrays, wind speeds in excess of 5 m s^{-1} reduced infrared heater efficiency at the same time that the energy requirement for warming increased (e.g., Kimball, 2005; Kimball *et al*., 2008, 2012a,b), and therefore, the efficacy of the aboveground plant warming was greatly reduced. Wind speeds were greater during daytime in open environments at both sites, which contributed to reduced midday ΔT^{above} in those conditions.

Although ambient and warmed plots did not track each other perfectly on a minute-by-minute basis because of environmental and technical challenges, we still achieved strong similarity in temperature patterns between ambient and heated plots (Figs 1, 6–9). The microenvironmental differences encountered among plots resulted from the spatial heterogeneity present in our forest sites and will challenge new forest warming arrays. Understanding microenvironmental patterns and integrating their dynamics into feedback control of warming would benefit future experimental designs within forested biomes.

Comparison of plant and air temperature

Our data show that ambient foliage and air temperatures had diurnal asynchrony (Fig. 10). Air temperature was generally cooler than foliage temperature at midday in our relatively humid environment with low evaporative demand. This is consistent with the pattern for vegetation to be cooler than air under high evaporative demand and to be warmer than air for small vapor pressure deficits (Idso *et al*., 1981). As expected, at nighttime, ambient foliage temperatures were below ambient air temperatures due to radiation to the cold night sky. Also as expected, foliage temperatures peaked in synchrony with solar radiation

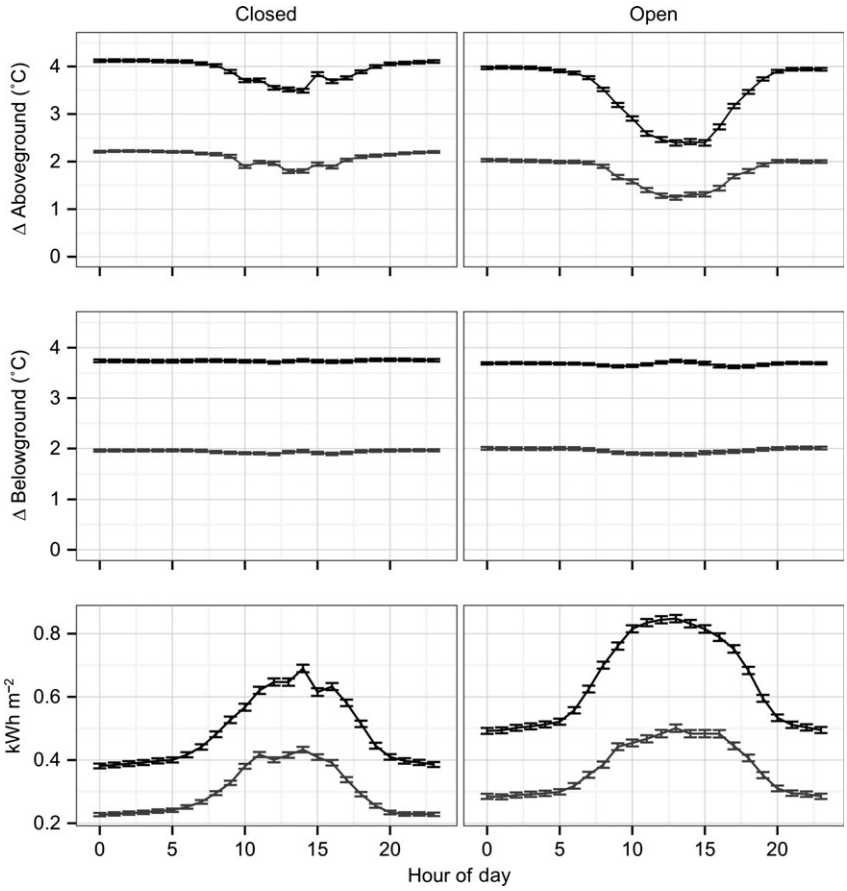

Fig. 9 Diurnal comparison of closed vs. open canopy sites by hour of day during field season; (row 1) ΔT (°C) for aboveground treatments for 2009–2010 by hour of day with 95% CI bars ($\Delta T^{1.7}$ (medium gray), and $\Delta T^{3.4}$ (dark gray)), (row 2) ΔT (°C) for belowground treatments (10-cm depth) for 2009–2011 by hour of day with 95% CI bars ($\Delta T_{1.7}$ (medium gray), and $\Delta T_{3.4}$ (dark gray)), and (row 3) mean kWh $m^{2\ -1}$ by hour of day.

Table 3 Mean (SE) belowground temperature and mean difference (SE) by depth during the 2011 field season sampling of CFC open plots comparing +3.4 °C and ambient treatments

Depth	$T_{3.4}$	T_{Amb}	$\Delta_{3.4}$
20 cm	14.88 (0.35)	11.41 (0.39)	3.47 (0.06)
30 cm	14.53 (0.34)	11.36 (0.37)	3.18 (0.05)
50 cm	13.84 (0.33)	11.24 (0.34)	2.6 (0.05)
75 cm	12.96 (0.31)	10.89 (0.32)	2.07 (0.02)
100 cm	12.26 (0.3)	10.62 (0.3)	1.64 (0.02)

while air temperatures peaked later. This asynchrony contributed to the need for additional energy from IR heaters in midday. In the time between the peak in foliage temperature and air temperature, gradients between foliage and surrounding air are greatest, especially in windy conditions. This also caused diurnal fluctuations to be greater in open canopy than closed canopy (Fig. 10). These observations complicate direct comparisons of diurnal patterns of temperature in air- vs. foliage-based warming experiments. Supplementary air temperature data show some stratification in air temperature exists with height in both ambient and elevated plots (Fig. S5). Our data also show that observed air temperature increases from IR heaters is dynamic, like foliage temperature, and relate to daily climate conditions such as wind (Fig. S6).

Applications and explorations

The forest environment, experimental constraints, and the growth of vegetation interacted to create the observed diurnal and seasonal differences in treatment efficiency and efficacy. Nonetheless, the approaches used in this experiment provided consistent differences (near targets) between ambient and warmed plots across open and closed canopy environments and

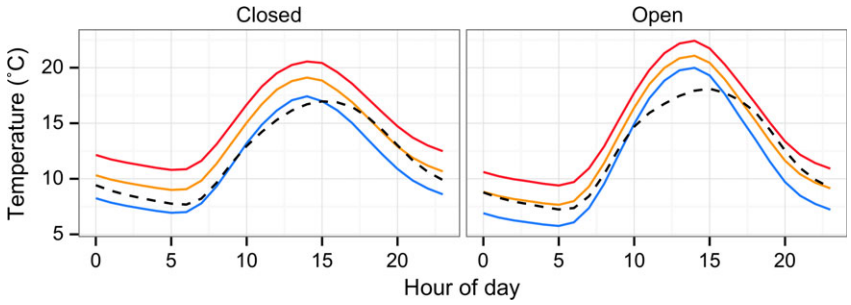

Fig. 10 Observed diurnal relationship between mean ambient air temperature (dashed black) and mean foliage temperatures in for T^{amb} (blue), $T^{1.7}$ (orange), and $T^{3.4}$ (red) across 2009–2011 field seasons.

mimicked the diurnal and annual differences in ΔT associated with projected future warming (Figs 6–8).

Growth of the seedling canopy also contributed to lower midday diurnal efficacy, given the maximum heating capacity of our experimental facility. As vegetation height and total leaf area increased with time, the heaters became relatively more underpowered. Power consumption necessary to achieve a fixed temperature elevation increased with leaf expansion and diminished with senescence (Fig. 8). This was most acute in open canopy +3.4 °C plots at CFC in 2011, where seedlings were growing fastest. Moreover, our +3.4 °C treatments were underpowered on an area basis as compared to the +1.7 °C treatments, not surprising given that there were six heaters per plot in the latter treatment and eight in the former. The need to increase heater height to accommodate a taller canopy also reduced efficiency over time. These limitations could be overcome by adding additional warming infrastructure in each plot.

The soil warming infrastructure proved to be efficient and may have buffered variation in aboveground heating. Although we have no experimental comparison of aboveground-only vs. belowground-only heating in this experimental design (except during periods when one of the systems was manually shut off), comparing the observations of the IR heaters' effects on soils with and without foliage (from early spring and late fall observations vs. midsummer observations) is instructive. Soil heating was nearly unnecessary at 10 cm depth in the early spring each year until leaf expansion had occurred. However, increased foliage abundance reduced the ability to reach soil heating targets at 10 cm depth using only the IR heaters. Our soil resistance cables used more power early in the day and soil thermal capacity allowed soils to maintain their differential through diurnal temperature declines at night. HWRC soils required more power outputs than those at CFC, which may be related to soil textural differences. Overall, belowground power was ~ 2% of that used aboveground in large part because the soil's thermal mass retained heat once soil temperature was elevated. Soil warming did not uniformly reach target elevations with increasing depth (Table 3, Fig. S3), but it represents an improvement with respect to deep soil warming as compared to aboveground-only experiments. However, as we were only able to measure deep soil warming 1 m from the plot edge, it is logical that soils closer to plot edges would have less warming at depth due to cooler (ambient temperature) surrounding soils.

Infrared warming experiments without soil warming cables (Nijs *et al.*, 2000; Kimball *et al.*, 2008; Luo *et al.*, 2010; Morgan *et al.*, 2011; Wall *et al.*, 2013; LeCain *et al.*, 2014; and McDaniel *et al.*, 2014) have reported significant soil warming primarily at shallow depths (less than 10 cm). However, the warming effects of IR heaters alone are likely reduced in dense vegetation and high moisture soils. Moreover, the effects may depend on the proportion of soil area directly intercepting reflected IR radiation, especially in smaller plots surrounded by soils and vegetation at ambient temperature. We also did not observe the decline in soil warming with increasing soil moisture that has been seen in aboveground-only experiments (data not shown). Overall, belowground warming is useful in achieving warming at deeper depths, resulting in a more ecologically realistic temperature depth profile (i.e., consistent with historical field measurements of soil temperature x depth observations in boreal soils; Qian *et al.*, 2011).

Adding belowground warming should be considered when IR heaters or aboveground heating would not adequately heat soils to match expectations in a warmer climate; characteristics of these ecosystems would include wet soils, deep soils and/or deeply rooted vegetation, dense vegetation, or deep litter layers. The depth of warming and technique deployed should be scaled to the rooting depth of the ecosystem. As this experiment's original design and belowground soil

warming methods have seen several innovations, Hanson *et al*. (2011) installed a ring of vertically oriented soil heaters around the periphery of their chambers to warm at deeper depths than this study. Also, a current experiment in perennial grasslands uses minimal impact 10 mm diameter vertical warming pins within plots to maintain 2.5 °C temperature elevations to 1 m depth with minimal initial soil disturbance (*Rich et al*., unpublished). Horizontal cabling may be best deployed in ecosystems where temporary soil disturbance is not an issue, or where it is an aspect of the disturbance regime. Horizontal cabling is advantageous in complex soil profiles such where deeper methods would not be feasible. Deploying of soil warming should not be a financial constraint as the relative costs of heating belowground are much lower than aboveground.

Although we found some seasonal and diurnal variation in our ability to meet our target treatment levels, our achieved treatments match seasonal patterns of long-term climate change in northeastern Minnesota, where temperature elevations have also been lower in midsummer than in shoulder seasons and lower at day than night (Handler *et al*., 2014). Thus, our realized treatments better match historical warming than our target goals. Nonetheless, the lessons learned should allow others who use this technique to effectively deliver realistic warming treatments based on any target goal provided that adequate resources are allocated to the experimental design and energy needs. Concurrent aboveground foliage warming with soil warming has promising applicability across many ecosystems, including developing forests that have larger saplings, grassland, savannas, wetlands, and ecosystems that reach a stable or predictable vegetation height over the duration of the experiment.

Acknowledgements

Gratitude to the myriad and multitude of assistants, students, and colleagues who make large projects work and special thanks to Karen Rice, Kyle Gill, Kirk Wythers, Jacek Oleksyn, John Blanchard, Ron Severs, and Nate Russart. Funding provided by: U.S. Department of Energy Program on Ecological Research 385 Grant No. DE-FG02-07ER64456; University of Minnesota: College of Food, Agricultural, and Natural Resources Sciences; Wilderness Research Foundation; and Minnesota Department of Natural Resources.

References

Amthor JS, Hanson PJ, Norby RJ, Wullschleger SD (2010) A comment on "Appropriate experimental ecosystem warming methods by ecosystem, objective, and practicality" by Aronson and McNulty. *Agricultural and Forest Meteorology*, **150**, 497–498.

Aronson EL, McNulty SG (2009) Appropriate experimental ecosystem warming methods by ecosystem, objective, and practicality. *Agricultural and Forest Meteorology*, **149**, 1791–1799.

Bergh J, Linder S (1999) Effects of soil warming during spring on photosynthetic recovery in boreal Norway spruce stands. *Global Change Biology*, **5**, 245–253.

Bronson DR, Gower ST, Tanner M, Linder S, Van Herk I (2008) Response of soil surface CO_2 flux in a boreal forest to ecosystem warming. *Global Change Biology*, **14**, 856–867.

Bronson DR, Gower ST, Tanner M, Linder S, Van Herk I (2009) Effect of ecosystem warming on boreal black spruce bud burst and shoot growth. *Global Change Biology*, **15**, 1534–1543.

Frelich LE, Reich PB (1995) Spatial patterns and succession in a Minnesota southern boreal forest. *Ecological Monographs*, **65**, 325–346.

Gaihre YK, Wassmann R, Tirol-Padre A, Villegas-Pangga G, Aquino E, Kimball BA (2014) Seasonal assessment of greenhouse gas emissions from irrigated lowland rice fields under infrared warming. *Agriculture, Ecosystems, and Environment*, **184**, 88–100.

Grigal DF, Ohmann LF (1975) Classification, description, and dynamics of upland plant communities within a Minnesota wilderness area. *Ecological Monographs*, **45**, 389–407.

Handler S, Duveneck MJ, Iverson L *et al*. (2014) Minnesota Forest Ecosystem Vulnerability Assessment and Synthesis: A report from the Northwoods Climate Change Response Framework. Gen. Tech. Rep. NRS-XX. Newtown Square, PA; U.S. Department of Agriculture, Forest Service, Northern Research Station. Unpublished.

Hanson PJ, Childs KW, Wullschleger SD, Riggs JS, Thomas WK, Todd DE, Warren JM (2011) A method for experimental heating of intact soil profiles for application to climate change experiments. *Global Change Biology*, **17**, 1083–1096.

Harte J, Shaw R (1995) Shifting dominance within a montane vegetation community – results of a climate-warming experiment. *Science*, **267**, 876–880.

Harte J, Torn MS, Chang FR, Feifarek B, Kinzig AP, Shaw R, Shen K (1995) Global warming and soil microclimate – results from a meadow-warming Experiment. *Ecological Applications*, **5**, 132–150.

Heinselman ML (1973) Fire in the virgin forest of the boundary waters canoe area, Minnesota. *Journal of Quaternary Research*, **3**, 329–382.

Hollister RD, Webber PJ (2000) Biotic validation of small open-top chambers in a tundra ecosystem. *Global Change Biology*, **6**, 835–842.

Idso SB, Reginato RJ, Jackson RD, Pinter PJ (1981) Foliage and air temperatures – evidence for a dynamic equivalence point. *Agricultural Meteorology*, **24**, 223–226.

IPCC (2013) *Climate Change 2013: The Physical Science Basis. Contribution of Working Group I to the Fifth Assessment Report of the Intergovernmental Panel on Climate Change*. Cambridge University Press, Cambridge, UK and New York, NY USA.

Kimball BA (2005) Theory and performance of an infrared heater for ecosystem warming. *Global Change Biology*, **11**, 2041–2056.

Kimball BA (2011) Comment on the comment by Amthor *et al*. on "Appropriate experimental ecosystem warming methods" by Aronson and McNulty. *Agricultural and Forest Meteorology*, **151**, 420–424.

Kimball BA, Conley MM (2009) Infrared heater arrays for warming field plots scaled up to 5-m diameter. *Agricultural and Forest Meteorology*, **149**, 721–724.

Kimball BA, Conley MM, Wang S, Lin X, Luo C, Morgan J, Smith D (2008) Infrared heater arrays for warming ecosystem field plots. *Global Change Biology*, **14**, 309–320.

Kimball BA, Conley MM, Lewin KF (2012a) Performance and energy costs associated with scaling infrared heater arrays for warming field plots from 1 to 100 m. *Theoretical and Applied Climatology*, **108**, 247–265.

Kimball BA, White JW, Wall GW, Ottman MJ (2012b) Infrared-warmed and unwarmed wheat vegetation indices coalesce using canopy-temperature-based growing degree days. *Agronomy Journal*, **104**, 114–118.

Kling GW, Hayhoe K, Johnson LB *et al*. (eds.) (2003) *Confronting Climate Change in the Great Lakes Region: Impacts on our Communities and Ecosystems*. Union of Concerned Scientists and Ecological Society of America, Cambridge, MA.

LeCain D, Smith S, Morgan J, Kimball BA, Pendall E, Miglietta F (2014) *Microclimatic Performance of a Free-air Warming and CO_2 Enrichment Experiment in Windy Wyoming*. Methods in Ecology and Evolution (submitted), USA.

Luo C, Xu G, Chao Z *et al*. (2010) Effect of warming and grazing on litter mass loss and temperature sensitivity of litter and dung mass loss on the Tibetan plateau. *Global Change Biology*, **16**, 1606–1617.

Marion GM, Henry GHR, Freckman DW (1997) Open-top designs for manipulating field temperature in high-latitude ecosystems. *Global Change Biology*, **3**, 20–32.

McDaniel MD, Wagner RJ, Rollinson CR, Kimball BA, Kaye MW, Kaye JP (2014) Microclimate and ecological threshold responses in a warming and wetting experiment following whole tree harvest. *Theoretical and Applied Climatology*, **116**, 287–299.

Morgan JA, LeCain DR, Pendall E *et al*. (2011) C_4 grasses prosper as carbon dioxide eliminates desiccation in warmed semi-arid grassland. *Nature*, **476**, 202–206.

Nijs I, Kockelbergh F, Heuer M, Beyens L, Trappeniers K, Impens I (2000) Climate-warming simulation in tundra: enhanced precision and repeatability with an improved infrared-heating device. *Arctic, Antarctic, and Alpine Research*, **32**, 346–350.

Ochsner TE, Sauer TJ, Horton R (2007) Soil heat storage measurements in energy balance studies. *Agronomy Journal*, **99**, 311–319.

Ogée J, Lamaud E, Brunet Y, Berbigier P, Bonnefond JM (2001) A long-term study of soil heat flux under a forest canopy. *Agricultural and Forest Meteorology*, **106**, 173–186.

Ottman MJ, Kimball BA, White JW, Wall GW (2012) Wheat growth response to increased temperature from varied planting dates and supplemental infrared heating. *Agronomy Journal*, **104**, 7–16.

Peterjohn WT, Melillo JM, Bowles FP, Steudler PA (1993) Soil warming and trace gas fluxes – experimental-design and preliminary results. *Oecologia*, **93**, 18–24.

Peterjohn WT, Melillo JM, Steudler PA, Newkirk KM, Bowles FP, Aber JD (1994) Responses of trace gas fluxes and N availability to experimentally elevated soil temperatures. *Ecological Applications*, **4**, 617–625.

Qian B, Gregorich EG, Gameda S, Hopkins DW, Wang XL (2011) Observed soil temperature trends associated with climate change in Canada. *Journal of Geophysical Research-Atmospheres*, **116**, D02106.

Reich PB, Sendall KM, Rice K, Rich RL, Stefanski A, Hobbie SE, Montgomery RA (2015) Geographic range predicts photosynthetic and growth response to warming in co-occurring tree species. *Nature Climate Change*.

Rehmani MIA, Zhang J, Li G *et al*. (2011) Simulation of future global warming scenarios in rice paddies with open-field warming facility. *Plant Methods*, **7**, 41.

Ruiz-Vera UM, Siebers M, Gray SB *et al*. (2013) Global warming can negate the expected CO_2 stimulation in photosynthesis and productivity for soybean grown in the Midwestern United States. *Plant Physiology*, **162**, 410–423.

Rustad LE, Fernandez IJ (1998) Experimental soil warming effects on CO_2 and CH4 flux from a low elevation spruce-fir forest soil in Maine, USA. *Global Change Biology*, **4**, 597–605.

Sendall KM, Reich PB, Zhao C *et al*. (2014) Acclimation of photosynthetic temperature optima of temperate and boreal tree species in response to experimental forest warming. *Global Change Biology*, doi:10.1111/gcb.12781.

Sherwood S, Fu Q (2014) A drier future? *Science*, **343**, 737–739.

Verburg PSJ, Van Loon WKP, Lukewille A (1999) The CLIMEX soil-heating experiment: soil response after 2 years of treatment. *Biology and Fertility of Soils*, **28**, 271–276.

Wall GW, Kimball BA, White JW, Ottman MJ (2011) Gas exchange and water relations of spring wheat under full-season infrared warming. *Global Change Biology*, **17**, 2113–2133.

Wall GW, McLain JET, Kimball BA, White JW, Ottman MJ, Garcia RL (2013) Infrared warming affects intra-row soil carbon dioxide efflux during vegetative growth of spring wheat. *Agronomy Journal*, **105**, 607–618.

Wan S, Luo Y, Wallace LL (2002) Changes in microclimate induced by experimental warming and clipping in tallgrass prairie. *Global Change Biology*, **8**, 754–768.

Supporting Information

Additional Supporting Information may be found in the online version of this article:

Figure S1. Schematic of experimental site, block and plot layouts for B4WarmED. Cloquet Forestry Center (CFC) site has open blocks and closed canopy blocks contiguous to each other. At the Hubachek Wilderness Research Center (HWRC) closed canopy blocks are contiguous and open canopy occupy surrounding areas.
Figure S2. Schematic of aboveground and belowground feedback control systems for B4WarmED experiments.
Figure S3. Average daily belowground temperature by depth and day of year in 2011 CFC open plots (T_{amb} (blue), $T_{3.4}$ (red)).
Figure S4. Average field season volumetric water content (VWC, cm^3 H_2O/cm^3 soil) for T^{amb} (blue), $T^{1.7}$ (orange), and $T^{3.4}$ (red) by year and site (with 95% CI bars).
Figure S5. Example mean air temperature by a) height and b) distance from plot center for concurrently run $T^{3.4}$ (red) and T^{amb} (blue) plots in July 2011 with (SE bars).
Figure S6. Mean temperature elevation from ambient for air temperature (blue) and foliage temperature (green) by hourly wind speed (ms^{-1} with 95% CI bars) for $T^{1.7}$ (left) and $T^{3.4}$ (right).
Table S1. Aboveground annual and seasonal temperature differences between CFC and HWRC experiment sites.
Table S2. Summary of power costs and power use for HWRC and CFC sites from 2009–2011.
Table S3. Major components and sources used in B4WarmED feedback control system.
Table S4. Feedback Control Program Language written in CR-basic.
Table S5. Average warmed season aboveground temperature (°C) for T^{amb}, $T^{1.7}$, and $T^{3.4}$ by year and period of day for HWRC and CFC sites (with standard error).
Table S6. Average warmed season belowground temperature at 10-cm depth (°C) for T_{amb}, $T_{1.7}$, and $T_{3.4}$ by year and period of day for HWRC and CFC sites (with standard error).
Table S7. FLIR analysis by direction.